J Appl Electrochem (2011) 41:527–534
DOI 10.1007/s10800-011-0273-4

ORIGINAL PAPER

Platinum nanoparticles self-assembled onto chitosan membrane as anode for direct methanol fuel cell

Mehri-Saddat Ekrami-Kakhki · Mozhgan Khorasani-Motlagh · Meissam Noroozifar

Received: 23 November 2010 / Accepted: 4 February 2011 / Published online: 4 March 2011

Abstract In this article, incorporation of platinum nanoparticles (PtNPs) into chitosan-coated glassy carbon (GC) electrode for methanol oxidation is studied. Pt–chitosan nanocomposites are prepared and characterized by UV–vis spectroscopy, X-ray powder diffraction (XRD), and transmission electron microscopy (TEM). Catalytic activity of GC–PtNPs–chitosan electrode for the electrooxidation of methanol is studied by cyclic voltammetry and chronoamperometry. The current density and potential of the methanol oxidation are affected by amount of platinum, methanol, sulfuric acid, and chitosan. The current density of the methanol oxidation at GC–PtNPs–chitosan electrode is measured in optimized conditions and compared with that obtained at the glassy carbon modified electrode by Pt with different polymers.

Keywords Direct methanol full cell · Nanoparticles · Platinum · Chitosan · Electrocatalyst

1 Introduction

The direct methanol fuel cell (DMFC) has attracted much research attention over the past two decades due to its high theoretical energy density (4.8 kWh l^{-1}) and potential suitability as power source for both automotive transportation and portable electronic devices [1]. The necessity for liquid fuels for fuel cells arises from the complications related to hydrogen storage and distribution. Hydrogen has a low volumetric energy density at atmospheric pressure and conventional means of increasing its energy density through liquefaction or compression are either costly or too bulky for small-scale, portable electronic applications [2]. The use of methanol as energy carrier and its direct electrochemical oxidation in direct methanol fuel cells (DMFCs) represents an important challenge for the polymer electrolyte fuel cell technology, since the complete system would be simpler without a reformer and reactant treatment steps. The use of methanol as fuel has several advantages in comparison to hydrogen: it is a cheap liquid fuel, easily handled, transported, and stored, and with a high theoretical energy density [3–5]. Catalytic materials for the electrooxidation of methanol have been extensively researched due to the interest in the development of direct methanol fuel cells (DMFCs). The search for new and less expensive alternative materials as anodes for direct methanol fuel cells has been a topic of current interest [6]. To date, the most efficient methanol anodes are based on platinum and ruthenium [7, 8].

Dispersion of the platinum micro particles in polymer matrix [9, 10] or deposition of Pt layers on the less expensive metal materials [11] are the ways that reduced cost of anode materials in the fuel cell applications.

Incorporation of noble metal (e.g., Pt, Ru, Re, etc.) particles into conducting polymer-coated electrode, which exhibits enhanced electrocatalytic activities as compared with the bulk form metal electrode in the oxidation of methanol, has been studied [12–16]. The increase in the catalytic activity may be due to the decrease in the poising effect, which is caused by highly dispersed single metal [12, 13] and the synergistic effects of conducting polymer and metal particles [17, 18]. Moreover, the possibility of dispersing metallic particles inside these polymers gives electrodes with higher surface areas and enhanced

M.-S. Ekrami-Kakhki · M. Khorasani-Motlagh (✉) · M. Noroozifar
Department of Chemistry, University of Sistan & Baluchestan, P.O. Box 98155-147, Zahedan, Iran
e-mail: mkhorasani@chem.usb.ac.ir

electrocatalytic activities towards the oxidation of methanol. The conducting polymers used are mainly polyaniline [15, 16], polypyrrole [19, 20], and polythiophene [21, 22]. These polymers offer great advantages due to their very good conducting and mechanical properties and good adhesion to the electrode substrate.

Numerous studies have been performed on the preparation of new organic/inorganic hybrid materials and nanocomposites [23]. Polymers are considered as a good host material for metal [24–26]. Chitosan is a very abundant biopolymer obtained by the alkaline deacetylation of chitin (a polymer made up of acetylglucosamine units) which is one of the important natural polymers constituting the shells of crustaceans and the cell walls of many fungi. Chitosan is actually a heteropolymer containing both glucosamine units and acetylglucosamine units [27] (Fig. 1). Recently, much attention has been paid to chitosan as a potential polysaccharide resource due to its excellent properties, for example, the studies concerned with the blend films containing chitosan [28–31] based on its biocompatibility, biodegradability, nontoxicity, and adsorption properties. The presence of amine groups explains its unique properties among biopolymers: (a) its cationic behavior in acidic solutions, and (b) its affinity for metal ions. Metal ion sorption can occur through chelation mechanisms for metal cations in near neutral solutions or through electrostatic attraction and ion exchange for metal anions in acidic solutions [32]. While most studies focusing on the interactions of chitosan with metal ions were carried out to recover strategic metals or remove hazardous metals from dilute solutions, increasing attention has recently been paid to the manufacturing of elaborate materials based on metal–chitosan reactions. For example, several studies have expressed an interest in combining the effects of metal ions and chitosan for treating plant disease [33], manufacturing batteries [34–36], as well as manufacturing optical, and electronic devices [37, 38]. However, a growing number of articles have been published since the 1980s' in the field of chitosan for supported catalysis (or heterogeneous catalysis). There are many reasons for this recent interest in using chitosan for supporting catalytic metals: high sorption capacities, stability of metal anions (such as Pt and Pd) on chitosan, and physical (and chemical) versatility of the biopolymer. Among many polymer electrolyte membranes studied, chitosan membranes have shown a better performance for applications of low temperature fuel cells [39].

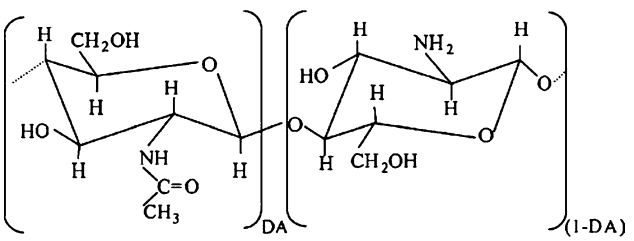

Fig. 1 Chitosan structure

In this study, the electrooxidation of methanol on the modified glassy carbon with Pt–chitosan nanocomposite electrode has been studied. Pt–chitosan nanocomposites were prepared by chemical reduction of corresponding metal ions into zero valent nanoparticles in the presence of chitosan. UV–vis spectra and transmission electron microscopy (TEM) images of the nanocomposites revealed the presence of metal nanoparticles. The electrochemical activity Pt–chitosan nanocomposites toward methanol were measured by cyclic voltammetry and chronoamperometry. The effect of various factors such as concentration of acid, methanol, chitosan, and nanoparticles amounts on the anodic current and potential of the methanol oxidation was studied and optimum value for each factor is suggested.

2 Experimental

2.1 Materials

Chitosan ([2-amino-2-deoxy-(1-4)-β-D-glucopyranose]), with medium molecular weight, 400,000 Da, was purchased from Fluka and used as received. H_2PtCl_6 and $NaBH_4$ were purchased from Merck, and used without further purification. Acetic acid was diluted to a 1% aqueous solution before use. All solutions were prepared using doubly distilled water. Purified N_2 (99.9%) was used without further treatment.

2.2 Characterization methods

UV–Vis spectra were recorded on an analytikjena SPECORD S100 spectrometer with photodiode array detector. X-ray powder diffraction (XRD) analysis was conducted on a Philips analytical PC-APD X-ray diffractometer with graphite monochromatic Cu Kα radiation ($\lambda = 1.54056$ Å) to verify the formation of products. TEM images were taken using a Philips CM120 transmission electron microscope with resolution 2.5 Å.

2.3 Preparation of Pt–chitosan nanocomposites

All glassware was thoroughly cleaned with freshly prepared aquaregain (3:1; HCl/HNO_3) and rinsed comprehensively with double-distilled water prior to use.

At first, a solution of chitosan (2 mg mL^{-1}) in 1% acetic acid solution was prepared, due to the poor solubility of chitosan, the mixture was stirred to completely dissolve and kept for overnight, and the solution was filtrated

through 0.22 m Millipore syringe filters to remove any impurity before use. The preparation of metal–chitosan nanocomposites is quite simple; a 25 μL H_2PtCl_6 aqueous solution (1 M) was mixed with 3 mL chitosan 1% (wt), the mixtures were stirred in a rotary (rpm 100) for 30 min. Then freshly prepared aqueous solution of $NaBH_4$ (50 μL, 2.4 M) as reducing agent was added quickly to the mixture, and kept stirring for another 90 min until the entire reduction of metal salts. The resulted nanocomposites (8.13×10^{-3} M of PtNPs) were kept at room temperature for characterization.

2.4 Electrochemical studies

Electrochemical measurements were carried out with an SAMA500 Electroanalyser (SAMA Research Center, Iran) controlled by a personal computer. All electrochemical experiments were carried out in a conventional three-electrode cell at room temperature. A platinum electrode and a saturated calomel electrode (SCE) were used as the counter and reference electrodes, respectively. All potentials were reported with respect to this reference electrode. The electrolyte solutions were deoxygenated with nitrogen bubbling before each voltammetric experiment. All experiments were performed under nitrogen atmosphere at room temperature. Scan rate for all experiment is 100 mV s^{-1}.

2.5 Electrode preparation, GC–PtNPs–chitosan

The glassy carbon (GC) working electrode with 3 mm of diameter (0.0706 cm^2) was polished with 0.05 μm alumina slurry to a mirror-finish. After rinsing with double-distilled water, it was sonicated in water and absolute ethanol for about 5 min each. Next, the GC electrode was transferred to the electrochemical cell for further cleaning and activation by using cyclic voltammetry between −1.5 and +1.5 V at a scan rate of 100 mV s^{-1} in freshly prepared deoxygenated 1.0 mol L^{-1} H_2SO_4 until a stable cyclic voltammetric profile (≈15 times) was obtained and then was used. 5 μL of the prepared PtNPs–chitosan suspension was spread by pipette onto the glassy carbon substrate. The subsequent evaporation of solvent led to the formation of the deposited catalyst layer.

3 Results and discussion

3.1 Characterization on Pt–chitosan nanocomposites

The structure of chitosan is like cellulose, which is an oxygen-rich natural carbohydrate (polysaccharide) consisting of anhydroglucose units joined by an oxygen linkage to form a linear molecular chain. When H_2PtCl_6 was mixed with chitosan solution, Pt(IV) ions could be bound to chitosan macromolecules probably via electrostatic (i.e., ion–dipole) interactions, because the electron-rich oxygen atoms of polar hydroxyl and ether groups of chitosan are expected to interact with electropositive transition metal cations. Pt nanoparticles were formed by reduction of Pt(IV) with $NaBH_4$ [40].

Figure 2 shows UV–Vis spectra of H_2PtCl_6 and prepared Pt–chitosan nanocomposites with chitosan solution as the reference. The absorption spectrum at 265 nm due to the absorption of Pt(IV) species [40] disappeared completely, indicating that Pt(IV) had been used up and colloidal Pt had been formed. As seen in Fig. 2b, for platinum nanoparticles, no plasmon absorbance could be observed between 300 and 800 nm this result is consistent with that reported by Yang et al. [41].

X-ray diffraction pattern of Pt in chitosan is depicted in Fig. 3, the XRD pattern confirms formation of platinum nanoparticles (JCPDS 04-0802). From the XRD data and Debye–Scherrer equation [42], the crystallite size of platinum nanoparticles was calculated 3.6 nm.

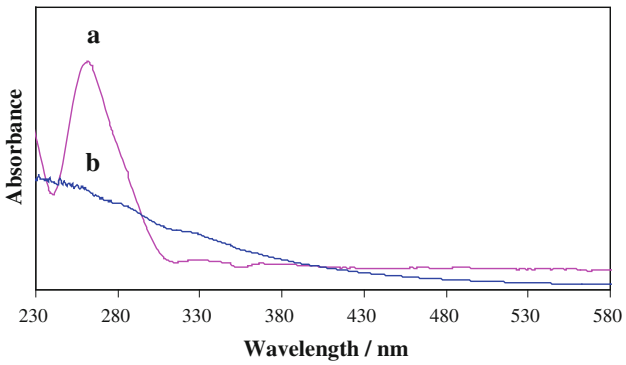

Fig. 2 UV–Vis spectra of (*a*) H_2PtCl_6 and (*b*) prepared Pt–chitosan nanocomposites

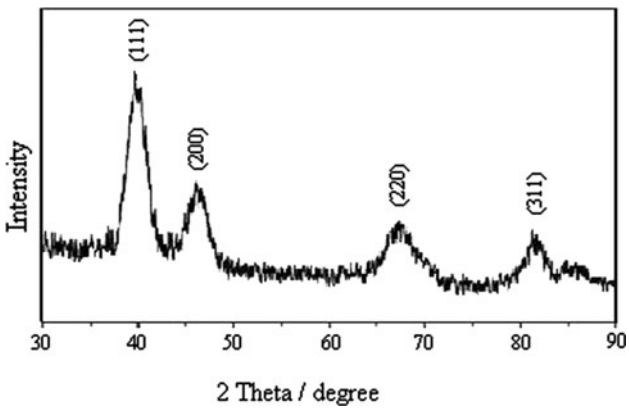

Fig. 3 XRD patterns of nanoparticles platinum in chitosan

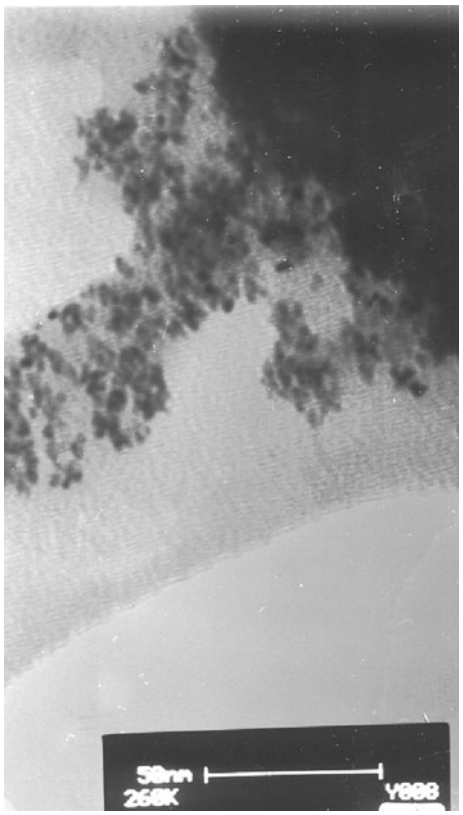

Fig. 4 Typical TEM image of prepared Pt–chitosan nanocomposites

The TEM image of prepared Pt–chitosan nanocomposite was shown in Fig. 4. The presence of Pt nanoparticles is clearly seen. It is seen from TEM image that the overall particle size of the platinum ranges from 2 to 7 nm and that particles exhibit fine spherical features.

3.2 Electrochemical characterization

The estimation of the electrochemical active surface area (EAS) can be made by cyclic voltammetry (CV) experiments in acid solution (N_2-saturated 0.125 M H_2SO_4 aqueous solution at room temperature). When the electrode potential is ramped linearly to a more positive potential (with respect to RHE) adsorbed hydrogen on Pt is oxidized to protons and electrons approximately in the 0–0.5 V range:

$$\text{Pt-H}_{ads} \leftrightarrow \text{Pt} + \text{H}^+ + \text{e}$$

While at higher potential Pt is first converted to Pt–OH and then to oxide. By decreasing the potential, the oxide is first reduced (approximately in the 0.5–1.0 V range) and at lower potential Pt–H_{ads} reforms. Due to the presence of different exposed crystalline faces for Pt particles, multiple peaks of direct and inverse reactions are usually observed. The EAS can be calculated from the CV curve, by calculation of the Coulombic charge for the hydrogen adsorption and desorption (Q_H) [43–45]. The value of Q_H (mC cm^{-2}) is the mean value between the amounts of charge transfer during the electroadsorption and desorption of H_2 on Pt sites [46], corrected by the contribution of double layer charge and eventually the support contribution. The EAS can be then calculated from Eq. 1:

$$\text{EAS} = \frac{Q_H}{0.21[\text{Pt}]} \quad (1)$$

where [Pt] represents the platinum loading (mg cm^{-2}) in the electrode, and 0.21 represent the charge required to oxidize a monolayer of H_2 on bright Pt [47].

Figure 5 displays the CV curves of the as-prepared catalysts in 0.125 M H_2SO_4 solution in the potential range of −0.8 to 1.2 V (vs. SCE). Well-defined CV feature of polycrystalline Pt is observed. There are two pairs of redox peaks around −0.011 and −0.311 V, which can be ascribed to hydrogen adsorption/desorption on crystal surface sites of Pt. The calculated EAS is 197.50 m^2 g^{-1} Pt for PtNPs–chitosan.

Cyclic voltammograms of modified GC with chitosan (GC–chitosan) and platinum–chitosan nanocomposites (GC–PtNPs–chitosan) were performed in the presence of methanol in potential range 0.0–1.8 V in 0.125 M H_2SO_4 and shown in Fig. 6. As seen in Fig. 6a, no oxidation peaks of methanol can be observed at GC–chitosan electrode (CV at GC electrode is not shown, which is similar to that of GC–chitosan electrode). This means that the GC and GC–chitosan have no electrocatalytic activity for methanol oxidation. The CV for methanol oxidation at the GC–PtNPs–chitosan indicates that there is a large increase in current during the forward scans. This indicates that PtNPs–chitosan is a good catalyst for methanol oxidation.

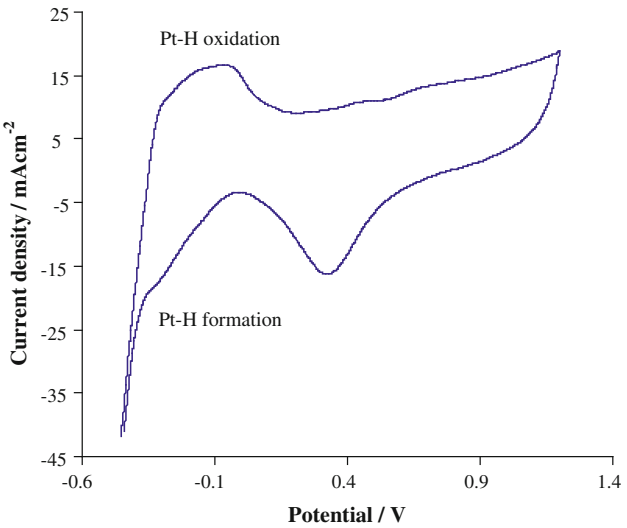

Fig. 5 Cyclic voltammogram of PtNPs catalysts in 0.125 M H_2SO_4 solution

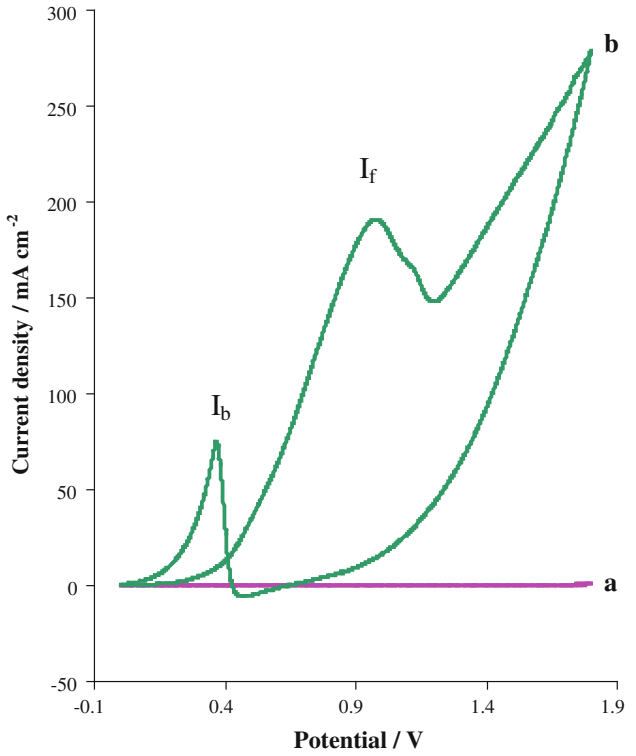

Fig. 6 Cyclic voltammograms for methanol oxidation in 0.125 M H_2SO_4 at (*a*) GC–chitosan and (*b*) GC–PtNPs–chitosan electrodes. (CV at GC electrode is not shown, which is similar to that of GC–chitosan electrode)

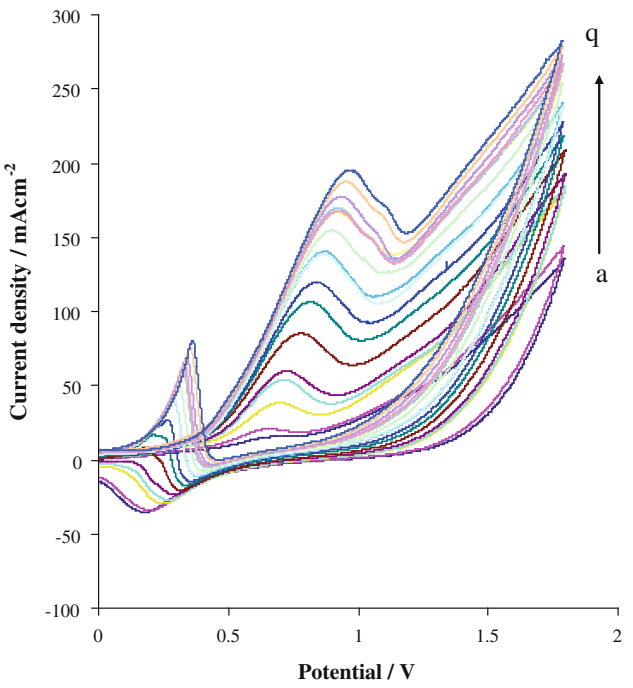

Fig. 7 Cyclic voltammograms for methanol oxidation at the GC–PtNPs–chitosan electrocatalyst in 0.125 M H_2SO_4 in different concentration of methanol: (*a*) 0.08, (*b*) 0.15, (*c*) 0.23, (*d*) 0.31, (*e*) 0.39, (*f*) 0.47, (*g*) 0.54, (*h*) 0.62, (*i*) 0.69, (*j*) 0.77, (*k*) 0.84, (*l*) 0.92, (*m*) 0.99, (*n*) 1.07, (*o*) 1.14, (*p*) 1.21, (*q*) 1.30 M

As seen from Fig. 6b, two oxidation peaks, which are related to the oxidation of methanol (I_f) and the corresponding intermediates (I_b) produced during the methanol oxidation ($I_f/I_b = 2.81$), can be observed obviously at 0.92 (E_f) and 0.35 V (E_b), respectively. The characteristics of the CV curves and the corresponding peak potentials (E_p) are in agreement with other works [48–51].

Figure 7 shows the effect of methanol concentration on the anodic current of methanol oxidation at the GC–PtNPs–chitosan. It is clearly observed that the anodic current increases with increasing methanol concentration and levels off at concentrations higher than 1.30 M. Also, when the methanol concentration increases from 0.08 to 1.30 M, the E_f and E_b shift towards positive direction from 0.66 to 0.92 V and 0.11 to 0.36 V, respectively. We assume this effect may due to the saturation of active sites on the surface of the electrode. And also, this indicates further that the electrooxidation of methanol at modified electrode is controlled by diffusion process. In accordance with this result, the optimum concentration of methanol to obtain a higher current density may be considered as about 1.30 M.

The effect of platinum amounts on the anodic current of methanol oxidation at the GC–PtNPs–chitosan was investigated by chronoamperometry in 1.30 M of methanol and 0.125 M H_2SO_4 at an anodic potential of 1.05 V vs. SCE

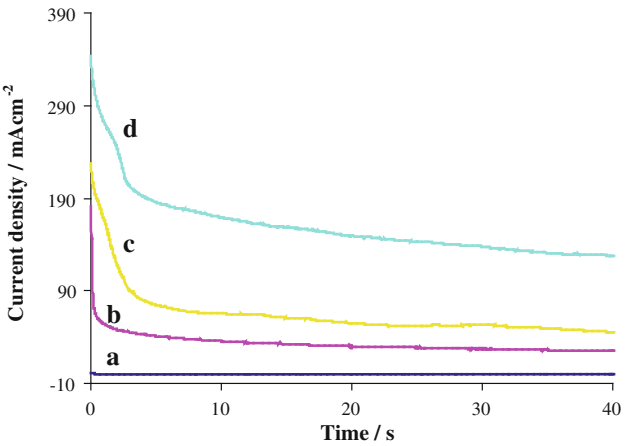

Fig. 8 Chronoamperometry for methanol oxidation at the GC–PtNPs–chitosan electrocatalyst in 0.125 M H_2SO_4 with different concentration of H_2PtCl_6: (*a*) 0, (*b*) 4, (*c*) 8, (*d*) 12 mM. (Chronoamperometry at GC electrode is not shown, which is similar to that of GC–chitosan electrode)

(Fig. 8). In all current–time curves for the GC–PtNPs–chitosan electrodes, there was an initial current drop in the first 7 s followed by a slower decay, but the current values obtained for the GC–PtNPs–chitosan eletrocatalysts were always higher than those obtained for GC and GC–chitosan electrocatalysts. Also, the current values increases considerably by increasing of Pt amounts. The data indicate that

the GC–PtNPs–chitosan catalysts have high activity for methanol oxidation as a pure GC and GC–chitosan sample yields zero current from the oxidation.

The experiments were done in different concentrations of sulfuric acid in the range of 0.03 to 1.0 M and the results are shown in Fig. 9. As seen in Fig. 9, the best result for the same amount of Pt is shown with sulfuric acid 0.125 M, so the experiments were done in this concentration of sulfuric acid.

The electrochemical oxidation of methanol at the GC–PtNPs–chitosan with different percentage of chitosan between 0.5 and 1.5%, has been investigated by cyclic voltammetry and the corresponding results are shown in Fig. 10. From Fig. 10, it can be observed that the anodic current (I_f) increases with the increase of chitosan and the maximum value of the peak current density is found at 1.0%. Then the I_f decreases with the further increase of chitosan. Therefore, chitosan% = 1.0% was chosen as optimum in acetic acid 1%.

The effect of anodic limit of potential scanning on the electrooxidation of methanol at GC–PtNPs–chitosan electrode was studied and the cyclic voltammograms obtained in the conditions that the final potential is varied between

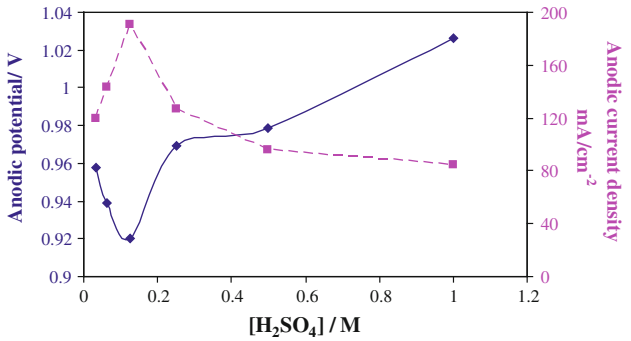

Fig. 9 Effect of acid concentration on the anodic current density (*dash line*) and potential (*solid line*) for methanol oxidation at the GC–PtNPs–chitosan electrode (1.30 M methanol, 1% chitosan)

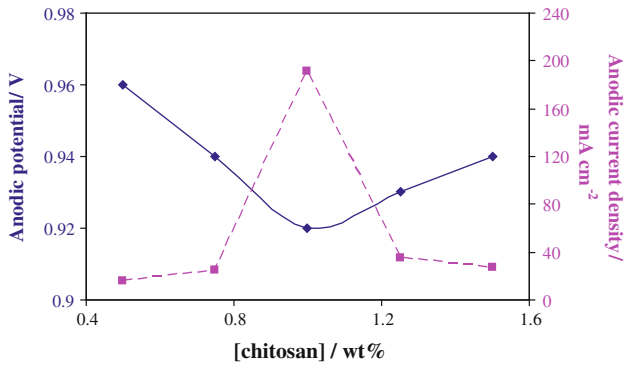

Fig. 10 Effect of chitosan% on the anodic current density (*dash line*) and potential (*solid line*) for methanol oxidation at the GC–PtNPs–chitosan electrode (1.30 M methanol, 0.125 M H_2SO_4)

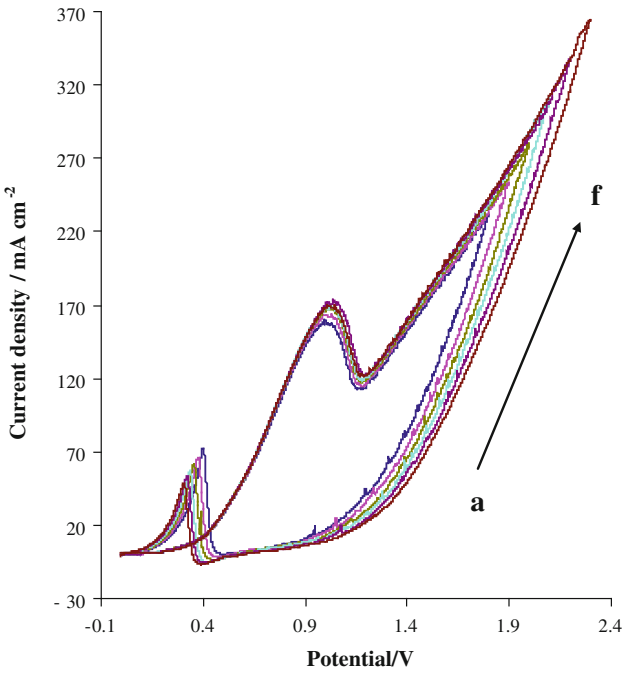

Fig. 11 Effect of upper limit of potential scanning region on the electrooxidation of 1 M methanol in 0.125 M H_2SO_4 at the GC–PtNPs–chitosan. (*a*) 1.8, (*b*) 1.9, (*c*) 2.0, (*d*) 2.1 (*e*) 2.2, (*f*) 2.3 V

1.8 and 2.3 V are shown for GC–PtNPs–chitosan electrode in Fig. 11. As seen in Fig. 11 by increasing the final positive potential limit, the anodic current of methanol oxidation (I_f) remains unchanged, but I_b is decreased. Indeed by increasing final positive potentials the conversion of Pt to PtO is accelerated and causes a decrease in I_b, which further demonstrates that methanol can only be oxidized on clean metallic platinum particles surface [52, 53].

Selected electrochemical data for methanol oxidation at GC-modified electrode with various catalysts are listed in Table 1 [54–58]. The oxidation current density at the GC–PtNPs–chitosan is considerably higher than that obtained at glassy carbon modified electrode by Pt with different polymers such as nafion, polyindole, and poly 5-methoxyindole. Electrochemical active surface area of the current study is also much more than that mentioned in Table 1, showing its higher catalytic activity toward methanol oxidation.

4 Conclusions

This research is aimed to increase the activity of anodic catalysts and thus to lower noble metal loading in anodes for methanol electrooxidation. We used dispersion of the platinum nanoparticles in chitosan matrix to reduce cost of anode materials. The GC–PtNPs–chitosan electrode was

Table 1 Electrochemical data for methanol oxidation on GC modified electrode with various catalysts

Catalyst composition	Onset methanol oxidation potential (V)	E_f (V)	I_f (mA cm^{-2})	Ref. electrode	Scan rate (mV s^{-1})	Electrolyte	EAS (m^2 g^{-1})	Ref.
Pt–EG-complex	0.3	0.64	65	SCE		2 M CH_3OH + 0.5 M H_2SO_4	83	[54]
Pt–EG–$NaBH_4$	0.3	0.64	50	SCE		2 M CH_3OH + 0.5 M H_2SO_4	70	[54]
Pt–CNT	0.2	0.8	16.1	SCE	50	2 M CH_3OH + 1 M H_2SO_4	86	[55]
Pt–MWCNT–alcohol–Nafion	0.20	0.69	19.19	SCE	100	2 M CH_3OH + 1 M H_2SO_4	107.9	[56]
Pt–PIn(polyindole)	0.15	0.70	60.17	SCE	50	1 M CH_3OH + 0.5 M H_2SO_4	34.52	[57]
Pt–PMI(poly 5 methoxyindole)	0.15	0.70	73.16	SCE	50	1 M CH_3OH + 0.5 M H_2SO_4	37.3	[57]
Pt–PPy(polypyrrole)	0.30	0.69	15.52	SCE	50	1 M CH_3OH + 0.5 M H_2SO_4	21.43	[57]
PtNPs–MWCNT	0.25	0.64	1.73	SCE	50	1 M CH_3OH + 1 M H_2SO_4	25.96	[58]
PtNPs–chitosan	0.18	0.92	190.47	SCE	100	1.3 M CH_3OH + 0.125 M H_2SO_4	197.50	This study

synthesized as active electrocatalyst for oxidation of methanol. Our results show the addition of chitosan into Pt catalysts can significantly improve the electrode performance for methanol electrooxidation. This polymer offers great advantages due to its nontoxicity and good adhesion to the electrode substrate. The increase in the catalytic activity towards the oxidation of methanol may be due to the decrease in the poisoning effect and the possibility of dispersing metallic particles inside chitosan gives electrodes with higher surface areas.

Acknowledgment We thank University of Sistan and Baluchestan (USB) for financial support.

References

1. Cheng TT, Gyenge EL (2008) J Appl Electrochem 38:51
2. Lam VWS, Alfantazi A, Gyenge EL (2009) J Appl Electrochem 39:1763
3. Lamy C, Lima A, LeRhun V et al (2002) J Power Sources 105:283
4. Hamnett A (1997) Catal Today 38:445
5. Reddington E, Sapienza A, Gurau B et al (1998) Science 280:1735
6. Witham CK, Chun W, Valdez TI et al (2000) Electrochem Solid-State Lett 3:497
7. Wasmus S, Kuver A (1999) J Electroanal Chem 461:14
8. Le′ger JM (2001) J Appl Electrochem 31:767
9. Golabi SM, Nozad A (2002) J Electroanal Chem 521:161
10. Golabi SM, Nozad A (2003) Electroanalysis 15:278
11. Foti G, Mousty C, Novy K et al (2000) J Appl Electrochem 30:147
12. Kost KM, Bartak DE, Kazee B et al (1988) Anal Chem 60:2379
13. Santhosh P, Gopalan A, Vasudevan T et al (2006) Appl Surf Sci 252:7964
14. Antolini E, Gonzalez ER (2009) Appl Catal A 365:1
15. Niu L, Li Q, Wei F et al (2005) J Electroanal Chem 578:331
16. Niu L, Li Q, Wei F et al (2003) Synth Met 139:271–276
17. Lenoe A, Marino W, Scharifker BR (1992) J Electrochem Soc 139:438
18. Zhong QL, Li WH, Tian ZQ (1994) Acta Physchim Sin 10:813
19. Bouzek K, Mangold K-M, Jüttner K (2001) J Appl Electrochem 31:501
20. Hammache H, Makhloufi L, Saidani B (2001) Synth Met 123:515
21. Biallozor S, Kupniewska A, Jasulaitene V (2003) Fuel Cells 3:8
22. Yassar A, Roncali J, Garnier F (1988) J Electroanal Chem 255:53
23. Mark JE (1996) Polym Eng Sci 36:2905
24. Akamatsu K, Takei S, Mizuhata M et al (2000) Thin Solid Films 359:55
25. Zeng R, Rong MZ, Zhang MQ et al (2002) Appl Surf Sci 187:239
26. Cole DH, Shull KR, Baldo P et al (1999) Macromolecules 32:771
27. Guibal E (2005) Prog Polym Sci 30:71
28. Du Y, Luo X-L, Xu J-J et al (2007) Bioelectrochemistry 70:342
29. Fuentes S, Retuert PJ, Ubilla A et al (2000) Biomacromolecules 1:239
30. Tanabe T, Okitsu N, Tachibana A et al (2002) Biomaterials 23:817–825
31. Zhang M, Li XH, Gong YD et al (2002) Biomaterials 23:2641
32. Guibal E (2004) Separ Purif Technol 38:43
33. Ben-Shalom N (2003) In: Brzezinski R, Boucher I, Retnakaran A (eds) Ninth international chitin–chitosan conference. Montreal, Canada
34. Mohamed NS, Subban RHY, Arof AK (1995) J Power Sources 56:153
35. Yahya MZA, Arof AK (2002) Eur Polym J 38:1191
36. Yahya MZA, Arof AK (2003) Eur Polym J 39:897
37. Yonezawa Y, Sato T, Kawabata I (1994) Chem Lett 23:355
38. Yonezawa Y, Kawabata I, Sato T (1996) Ber Bunsenges Phys Chem 100:39
39. Osifo PO, Masala A (2010) J Power Sources 195:4915

40. Tang Z, Geng D, Lu G (2005) Mater Lett 59:1567
41. Huang H, Yuan Q, Yang X (2004) Colloids Surfaces B 39:31
42. Ge X, Liu Y, Liu X (2001) Sens Actuators B 79:171
43. Cai K-D, Yin G-P, Wang J-J et al (2009) Energy Fuels 23:903
44. Saha MS, Li R, Sun X (2008) J Power Sources 7:314
45. Carter RN, Kocha SS, Wager FT et al (2007) ECS Trans 11(1):403
46. Pozio A, Francesco MD, Cemmi A et al (2002) J Power Sources 105:13
47. Maillard F, Martin M, Gloaguen F et al (2002) Electrochim Acta 47:431
48. Prater DN, Rusek JJ (2003) Appl Energy 74:135
49. Chen M, Wang ZB, Ding Y et al (2008) Electrochem Commun 10:443
50. Wang ZB, Zuo Pj, Yin GP (2009) J Alloys Compd 479:395
51. Razmi H, Habibi Es, Heidari H (2008) Electrochim Acta 53:8178–8185
52. Hu CC, Liu KY (1999) Electrochim Acta 44:2727
53. Nozad AG, Ghannadi MM, Sedaghat SS et al (2006) Electroanalysis 18:911
54. Kim P, Joo JB, Kim W et al (2006) J Power Sources 160:987
55. Saha MS, Li R, Sun X (2008) J Power Sources 177:314
56. Tong H, Li HL, Zhang XG (2007) Carbon 45:2424
57. Zhou W, Du Y, Ren F et al (2010) Int J Hydrog Energy 35:3270
58. Xu Y, Lin X (2007) Electrochim Acta 52:5140